Precision spectroscopy of HD at 1.38 μm

Eugenio Fasci, Antonio Castrillo, Hemanth Dinesan, Stefania Gravina, Luigi Moretti, and Livio Gianfrani*
Dipartimento di Matematica e Fisica, Università degli studi della Campania "Luigi Vanvitelli", Viale Lincoln 5, I-81100 Caserta, Italy

(Received 18 May 2018; published 22 August 2018)

The technique of frequency-stabilized comb-calibrated cavity ring-down spectroscopy was used to observe the weak R(1) transition of the deuturated molecular hydrogen (HD) first overtone band in the near infrared. Like molecular hydrogen, HD is a benchmark system to test quantum electrodynamics, looking for new physics beyond the standard model. The spectral line shape was measured with an extremely high fidelity at relatively low gas pressures. The use of a very refined line-shape model allowed us to retrieve the unperturbed line-center frequency of the R(1) line with a global uncertainty of about 100 kHz ($\delta\nu/\nu = 5\times10^{-10}$). Our value may solve the ambiguity that recently emerged for this line from a pair of sub-Doppler experiments. We also determined other parameters of interest, such as the line strength, the transition dipole moment, and the pressure-broadening coefficient.

DOI: 10.1103/PhysRevA.98.022516

I. INTRODUCTION

Deuterated molecular hydrogen (HD) is the simplest heteronuclear (and neutral) diatomic molecule, which has gained a growing interest in recent years for a variety of reasons. HD has been the subject of many astrophysical studies. Detection of HD lines from the interstellar medium in galaxies provides useful constraints on physical conditions, due to the fact that HD is fragile and easily photodissociated [1]. Moreover, the spectroscopic observation of HD aimed to estimate its abundance in the remote Universe is of the utmost importance in modern cosmology, as it provides important constraints on the baryonic matter density, thus testing the current assumptions on primordial nucleosynthesis in the very early universe [2]. HD is also involved in many fundamental measurements. Its electronic transitions have been used as a probe for detecting the proton-electron mass ratio on a cosmological timescale [3], while highly accurate laboratory measurements of line-center frequencies can be interpreted to put constraints on the strengths of putative fifth forces in nature, looking for new physics beyond the standard model [4]. Similarly, the nuclear magnetic resonance spectrum enables one to investigate the short-range spin-dependent interactions between protons and deuterons at the Å scale [5].

The HD infrared spectrum exhibits very weak electric dipole transitions and even weaker electric quadrupole components. The small electric dipole moment ($\approx$20 μD) is due to breaking of inversion symmetry in conjunction with the breakdown of the Born-Oppenheimer approximation. The first observation of the electric dipole spectrum of HD dates back to 1950, when Herzberg used a long-path technique to detect a few components of the second and third overtone bands [6]. Recently, extensive measurements have been performed by using cavity ring-down spectroscopy (CRDS) in the continuous-wave (cw) regime [7]. From the theory side, we have recently seen significant progress regarding the calculation capabilities in the framework of quantum electrodynamics. Consequently, rovibrational energy levels of HD have been calculated with high accuracy by including nonadiabatic, relativistic, and quantum electrodynamic effects, as well as finite nuclear size corrections [8]. Similarly, accurate calculations of transition dipole moments are also possible [9].

In this work, we report on the determination of the line-center frequency of the R(1) transition belonging to the first overtone vibrational band of HD, by using frequency-stabilized CRDS, assisted by a self-referenced fiber-laser-based frequency comb. Very recently, this line has been the subject of two sub-Doppler investigations: the former is based upon the observation of saturated absorption by means of the technique of noise-immune cavity-enhanced optical heterodyne molecular spectroscopy [10], and the latter exploits a comb-locked CRDS technique to perform Lamb-dip spectroscopy [11]. The two measurements of the line-center frequency present a disagreement of 0.895 MHz, larger than the uncertainty of each determination. In both experiments, the probe radiation intensity approached the level of 10^7 W/cm^2. This work is aimed to provide a third comb-calibrated measurement for the R(1) line under a linear regime of laser-gas interaction so that any perturbation arising from the light power could be avoided. The use of the CRDS technique enabled us to obtain a relatively high signal-to-noise ratio (SNR) at low pressures (smaller than 1500 Pa), a circumstance that leads to a good accuracy level even in the Doppler-limited regime.

II. EXPERIMENTAL APPARATUS

A schematic diagram of the experimental apparatus is shown in Fig. 1. The probe laser (PL) was an extended-cavity diode laser (ECDL) with an emission wavelength in the range between 1.38 and 1.41 μm. It was phase locked to a reference laser (RL), as already described elsewhere [12]. The offset frequency between the two lasers, f_{RF}, was provided by a radio-frequency synthesizer, which in turn was phase locked to a Rb clock. The reference laser was an ECDL, tightly

*Corresponding author: livio.gianfrani@unicampania.it

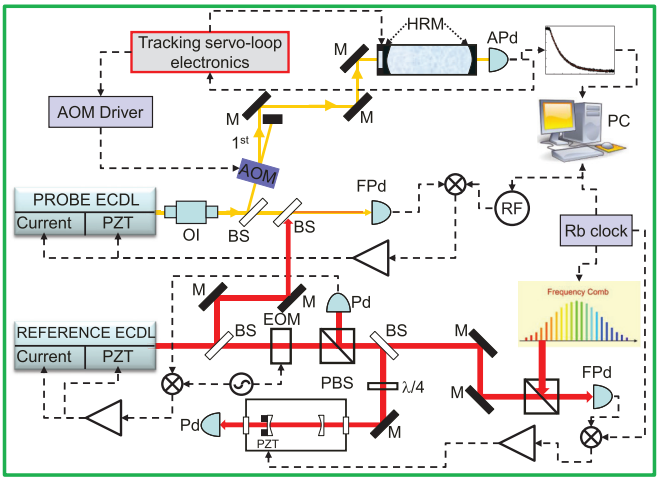

FIG. 1. Schematic diagram of the experimental setup. OI: optical isolator; BS: beam splitter; M: mirror; PBS: polarizing beam splitter; $\lambda/4$: quarter wave plate; PZT: piezoelectric transducer; AOM: acoustic-optic modulator; EOM: electro-optic modulator; HRM: high-reflectivity mirrors; FPd: fast photodiode; APd: avalanche photodiode; RF: radio-frequency synthesizer; PC: personal computer.

locked to a high-finesse cavity by means of the Pound-Drever-Hall technique so as to narrow its emission linewidth down to 7 kHz for an observation time of 1 ms [13]. In turn, the optical cavity was locked to one of the teeth of a self-referenced fiber-laser-based frequency comb (MenloSystems, model FC1500-250-ULN) in order to provide an absolute calibration of the frequency axis underneath the spectra. This latter was produced through an accurate and fine tuning of f_{RF}. The in-loop relative stability of the RL frequency with respect to the optical frequency comb synthesizer (OFCS) was found to be 2×10^{-14} for an integration time of 1 s, as determined from an Allan deviation analysis. It is worth noting that this value does not include the frequency drifts of the Rb clock to which the OFCS was referenced. The comb-calibrated dual-laser approach was preferred to the one in which the probe laser is directly referenced to the OFCS, due to the relatively large width of each comb tooth (of about 100 kHz). The RL absolute frequency is given by $f_{RL} = n\times f_{rep} \pm f_{ceo} \pm f_{beat}$, with f_{ceo} being the carrier-envelope offset frequency (set to 20 MHz), f_{rep} the comb repetition rate (equal to 250 MHz), f_{beat} the beat note frequency between RL and the nearest tooth of the comb, and n the comb-tooth order. The correct signs of f_{ceo} and f_{beat} could be easily determined by slightly varying f_{rep} and f_{ceo} and observing the consequent variation of f_{beat}. On the other hand, the comb order was provided by a direct measurement of the RL wavelength by means of a wavemeter (not shown in Fig. 1), whose accuracy (≈30 MHz) was better than half the comb-mode spacing.

The optical cavity, which was used for the aims of CRDS measurements, consisted of two spherical mirrors mounted on a Zerodur block with a cylindrical hole around its axis. The position of one of the two mirrors could be finely adjusted by means of a piezoelectric transducer. The cavity length was equal to 43 cm. The Zerodur spacer was equipped with three stainless-steel vacuum feedthroughs, which were used to create high-vacuum conditions into the cavity by means of a turbomolecular pump, to house an absolute pressure gauge (MKS Baratron, model 690A12TRA, with a full scale of 100 Torr and an accuracy of 0.05%), and to inlet the gas sample. The cavity was also equipped with a calibrated pt-100 thermometer with an accuracy of about 0.05% at room temperature. The empty cavity finesse was measured to be about 160 000, while the intracavity power was estimated to be ≈100 mW. A portion of the PL beam passed through an acousto-optic modulator (AOM) driven at a frequency f_{AOM} of 80 MHz. After spatial filtering by a 1-m-long polarization-maintaining optical fiber, the first-order diffracted beam was injected into the cavity. The AOM was used as an optical shutter for initiating the passive decay of the intracavity light. The ring-down events were monitored by means of an InGaAs avalanche detector, showing a noise equivalent power of 0.46 $pW/\sqrt{Hz}$ and a detection bandwidth of 420 kHz. The dc signal from the detector was digitized by a data acquisition board with a rate of 10^7 samples/s and a vertical resolution of 16 bit. For each ring-down event, 7000 points were recorded. For the aims of high-resolution cw-CRDS, a tracking servo-loop circuit was implemented so that the cavity could follow the probe laser while scanning the laser frequency around the absorption line of interest. The scheme of Ref. [14] was adopted, consisting of a ramp generator, a threshold detector, and a microcontroller unit. High-quality absorption spectra could be recorded in this way, characterized by an absolute frequency axis and an arbitrarily large number of points. For each point, the PL frequency could be determined through the following equation: $f_{PL} = f_{AOM} \pm f_{RF} + f_{RL} = f_{AOM} \pm f_{RF} + n\times f_{rep} \pm f_{ceo} \pm f_{beat}$. Here, the ambiguity on the sign of f_{RF} could be removed by comparing the PL wavelength with the RL one. Spectroscopic measurements were performed at room temperature by using a HD gas bottle with a ^{2}H-enrichment factor of 97% and a chemical purity of 98%. The explored pressure range goes roughly from 100 to 1500 Pa, corresponding to peak absorption coefficients between 10^{-7} and 2×10^{-6} cm^{-1}. The spectral line shape is essentially broadened by the Doppler effect, with the Doppler width being ≈1.5 GHz. A single run of measurements consists of 13 spectral acquisitions, one for each pressure value. In turn, individual spectra consist of 540 data points with a frequency step of 10 MHz. For each point, the decay time is given by the mean value over five consecutive ring-down events that leads to an acquisition time of about 0.3 s. Therefore, a single spectrum is acquired in about 3 minutes. In order to limit as much as possible gas contamination due to the interaction of the HD sample with the cell walls and to maintain high-purity conditions, the cell is evacuated by the turbomolecular pump after each spectral acquisition and filled again at the desired pressure. For that reason, a complete set of measurements typically requires the time span of a few hours. The spectroscopic measurements were repeated over 10 different days.

III. RESULTS AND DISCUSSION

Figure 2 reports an example of a complete set of measurements, along with fit residuals for the spectra at the lowest [Fig. 2(c)] and highest [Fig. 2(d)] pressure values. The SNR varied between 200 and 1000. These numbers are consistent

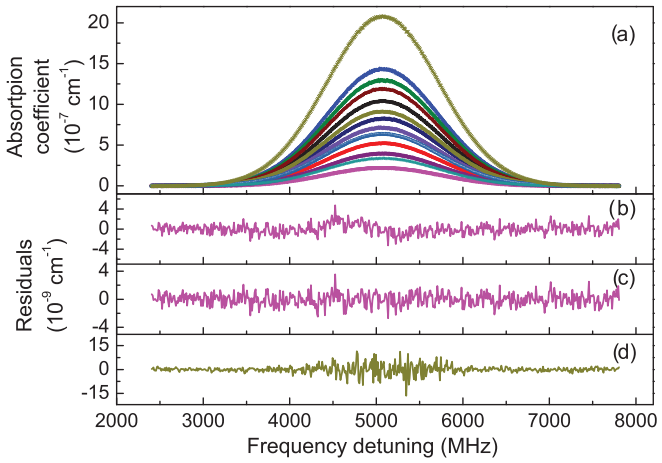

FIG. 2. (a) HD absorption spectra recorded at 13 different pressures, from 150 to 1400 Pa. (b) Residuals of the HD spectrum at the lowest gas pressure obtained without adding the HDO interfering line in the fitting procedure. (c), (d) Residuals at the lowest and highest pressures, respectively, including the HDO line.

with a detection sensitivity of $\approx 5\times10^{-10}$ cm$^{-1}/\sqrt{\text{Hz}}$. The choice of the line-shape model required particular care. As demonstrated elsewhere, collision-induced line-shape effects can limit the accuracy in Doppler-limited spectroscopy [15]. Furthermore, when the gas pressure approaches the atmospheric value, the extrapolation of the line position to zero pressure leads to a systematic shift that is due to the nonlinear behavior of the line-center frequency at high pressures [15]. For this reason, we decided to keep the HD pressure as small as possible, taking advantage of the high-detection sensitivity. We adopted the partially correlated quadratic speed-dependent hard-collision model, namely, the so-called Hartmann-Tran profile (HTP) [16]. This profile is sophisticated enough to capture the various collisional perturbations to the isolated line shape, accounting for the speed dependence of collisional broadening and shifting, Dicke narrowing effects, and the partial correlation between dephasing collisions and velocity-changing collisions. Moreover, the HTP implementation provided by Ngo *et al.* [17], in terms of the complex probability function, requires a small computation effort and, therefore, can be efficiently integrated into a fitting routine.

Relevant quantities of the HTP profile include the following: the most probable speed of the absorbing molecules of mass m that is given by $\overline{v} = \sqrt{\frac{2k_BT}{m}}$, with k_B being the Boltzmann constant, and T the thermodynamic temperature; the velocity-changing collision frequency, β; and the complex dephasing collision frequency, given by $\Gamma + i\Delta$, where Γ and Δ are the collisional broadening and shifting parameter, respectively. This latter quantity is modeled by using the quadratic approximation, as expressed by the following equation [18]:

$$\Gamma(v) + i\Delta(v) = (\Gamma_0 + i\Delta_0) + (\Gamma_2 + i\Delta_2)\left[\left(\frac{v}{\overline{v}}\right)^2 + \frac{3}{2}\right],$$

where Γ_0 and Δ_0 are the mean value of collisional broadening and shifting parameters (averaged over molecular speeds), while Γ_2 and Δ_2 are the coefficients accounting for the quadratic dependence. In turn, Γ_2 and Δ_2 can be written as $\Gamma_2 = a_w\Gamma_0$ and $\Delta_2 = a_s\Delta_0$, where a_w and a_s can be related to the intermolecular potential by means of the confluent hypergeometric function [18]. Finally, the temporal correlation between velocity changing collisions and dipole dephasing collisions is taken into account through the correlation parameter η. In this framework, the normalized HTP implementation, as a function of the angular frequency ω of the incident radiation can be written as

$$F_{\text{HTP}}(\omega) = \frac{1}{\pi}\text{Re}\left\{\frac{A(\omega)}{1 - [\beta - \eta(C_0 - 2C_2/2)]A(\omega) + (\eta C_2/\overline{v}^2)B(\omega)}\right\},$$

where $C_0 = \Gamma_0 + i\Delta_0$ and $C_2 = \Gamma_2 + i\Delta_2$. The terms $A(\omega)$ and $B(\omega)$ are given by

$$A(\omega) = \int \frac{f_{MB}(\mathbf{v})}{i(\omega - \omega_0 - \mathbf{k}\cdot\mathbf{v}) + (1-\eta)\left\{C_0 + C_2\left[\left(\frac{v}{\overline{v}}\right)^2 - \frac{3}{2}\right]\right\} + \beta} d\mathbf{v},$$

$$B(\omega) = \int \frac{v^2 f_{MB}(\mathbf{v})}{i(\omega - \omega_0 - \mathbf{k}\cdot\mathbf{v}) + (1-\eta)\left\{C_0 + C_2\left[\left(\frac{v}{\overline{v}}\right)^2 - \frac{3}{2}\right]\right\} + \beta} d\mathbf{v},$$

where $f_{MB}(\mathbf{v})$ is the Maxwell-Boltzmann distribution.

Finally, the absorption coefficient is given by $\alpha(\omega) = (P_0 + P_1\omega)\alpha_{\text{tot}}F_{\text{HTP}}(\omega)$, where P_0 and P_1 are a pair of parameters taking into account background variations of an instrumental nature, while α_{tot} is the integrated absorption coefficient. This is the complete function to which the experimental profiles were compared. Specifically, the CRDS spectra were analyzed by means of a nonlinear least-squares multispectrum fitting procedure. Without entering into the details, we underline that this procedure allows one to easily implement physical constraints among the HTP parameters, thus leading to a more accurate evaluation of them [19]. It also reduces the statistical correlation among the free parameters. In fact, Γ_0 and Δ_0 have a linear dependence on the pressure and, hence, on α_{tot}. On the other hand, a_w and a_s can be considered constant in the entire pressure range; consequently, these two parameters are shared among the various spectra of a single dataset. Other shared parameters are the zero-pressure line-center frequency, the velocity-changing collision frequency per unit pressure, the η parameter, and the pressure-broadening and -shifting coefficients. Instead, free parameters characteristic

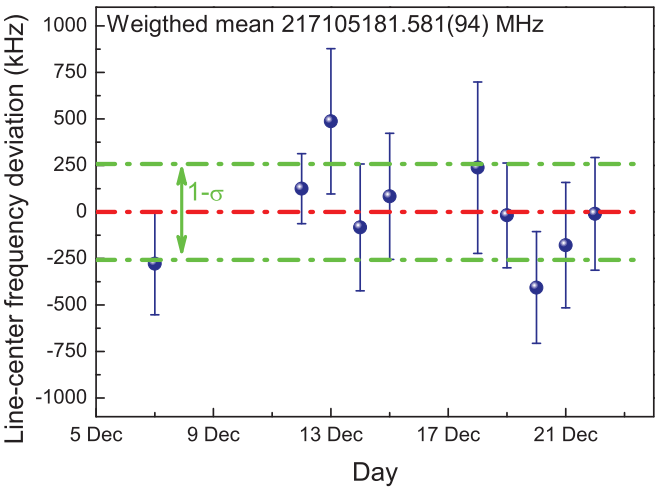

FIG. 3. Frequency deviations from the mean value as a result of repeated determinations of the R(1) frequency. The region marked by the green dash-dotted lines indicates the 1-σ standard deviation of the 10 different values.

of individual spectra are P_0, P_1, and $\alpha_{\rm tot}$. The Doppler width was set to the value corresponding to the cell's temperature.

The HD spectra are perturbed by a HDO transition (the $2_{2,0} \rightarrow 2_{2,1}$ line of the $2\nu_3$ band) whose center frequency is about 410 MHz away (at lower frequencies) from the R(1) line. The spectral analysis had to take this line into account, despite the high purity of the HD sample. In fact, water desorption from the cell walls adds some water vapor to the gas sample, thus making visible the influence of the HDO line, as clearly shown in Fig. 2(b). Here, the fit residuals of the spectrum at the lowest pressure, as obtained without adding the water line in the fitting procedure, are plotted. These residuals demonstrate the occurrence of the perturbation from the overlapping HDO line. The fitting procedure was applied to 10 datasets, each of them consisting of 13 spectra. In each run, the fitting code managed 7020 points and 46 free parameters of the HD profiles. The perturbation of the HDO line was considered by adding a Voigt convolution, which increases the number of free parameters from 46 to 61. The zero-pressure frequency of the HDO line was fixed at the value of the high-resolution transmission molecular absorption (HITRAN) database [20].

The good reproducibility of the 10 datasets (that justifies the use of the weighted mean) is demonstrated in Fig. 3, where the deviations of the line-center frequency from the mean value are plotted. The weighted mean of the various determinations gives 217 105 181.581 $\pm$ 0.094 MHz. The relative statistical uncertainty amounts to 4×10^{-10}, which is a remarkable result for a broad line observed in a Doppler-limited experiment.

TABLE II. Uncertainty budget (in terms of absolute contributions, corresponding to 1-σ) for the R(1) center frequency.

Contribution	Type-A components (kHz)	Type-B components (kHz)
Reproducibility	94	
Line-shape model		54
Frequency calibration		5
HDO center frequency		<10
Detector nonlinearity		Negligible
Temperature uncertainty and drifts		7
Hyperfine structure effects		Negligible
ac-Stark shift		<1
Overall uncertainty = 109 kHz		

In Table I, we report the other parameters of interest that are determined in the present study. Also in this case, the weighted means over the results of 10 datasets were performed. The determination of the line strength at the operation temperature ($T \approx 298$ K), $S(T)$, is based on the fact that the integrated absorption coefficient can be expressed as $\alpha_{\rm tot} = S(T)\times N$, where N is the molecular number density that is given by $0.97\times0.98\times\frac{p}{k_B T}$, with p being the gas pressure. For a comparison with the HITRAN database [20], the line-strength value was properly rescaled at the reference temperature of 296 K. The measured line strength shows a relative deviation from that of Ref. [7] of about -3%, while it presents a better agreement with the HITRAN value. The electric dipole transition moment μ was retrieved from the line strength using the expression of Ref. [21], while the partition function was calculated from the data of Ref. [8]. Our value of $2.105(3)\times10^{-5}$ D well compares with the theoretical one (2.122×10^{-5} D) [9], with the relative deviation being -1.1%.

It is worth noting that our values for the pressure-broadening and -shifting coefficients do not agree with those of Ref. [10], which, on the other hand, appear unrealistically large. This discrepancy might be due to the fact that the sub-Doppler experiment monitors collisional effects on a particular class of molecules, namely, those traveling in the plane orthogonal to the light beam. However, our pressure-broadening value is close to the one of the HITRAN database [20]. Table II gives the complete uncertainty budget for the absolute measurement of the line-center frequency. Apart from the uncertainty of statistical nature (type A), the main source of error is associated

TABLE I. Spectroscopic parameters of the R(1) line as measured in the present work and their comparison with previous determinations.

	This work	Values from Ref. [7]	HITRAN values [20]
Pressure-broadening coefficient (kHz/Pa)	9.76 $\pm$ 0.17		14.8
Pressure-shifting coefficient (kHz/Pa)	-0.44 $\pm$ 0.07		
Line strength (10^{-25} cm/molecule)	3.475 $\pm$ 0.004	3.577[a]	3.526

[a]at $T = 294$ K.

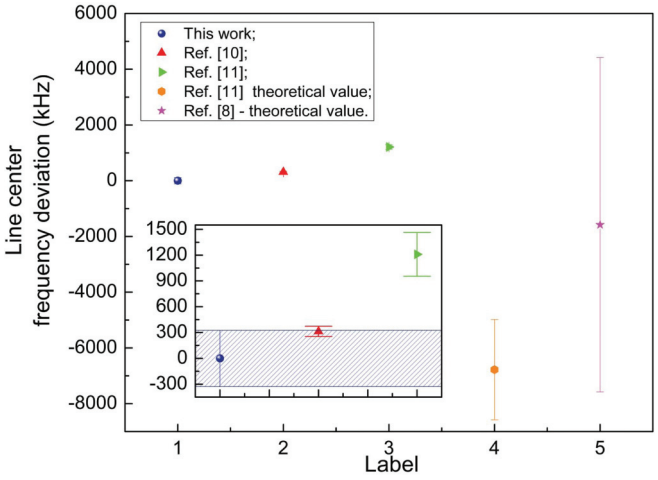

FIG. 4. Comparison among different experimental and theoretical values of the R(1) center frequency. The inset is a zoom on our value and on the recent sub-Doppler determinations.

to the line-shape model. In order to quote this contribution, the spectral analysis was repeated by adopting simplified line-shape models. First, since the η parameter was found to be consistent with zero, we repeated the fits by setting $\eta = 0$. Then, we tested the symmetric version of the quadratic speed-dependent hard-collision model (forcing Δ_2 to be equal to 0), with and without a partial correlation (namely, leaving η as a free parameter and setting $\eta = 0$). Finally, for those models accounting for the partial correlation between velocity-changing and dephasing collisions, the spectral analysis was also done by setting η equal to the quite usual value of 0.2. As expected, the lowest reduced chi-square (χ^2) was found for the most sophisticated profile, namely, the HTP model with all the parameters considered as variable quantities (except for the Doppler width). In a very prudent way, the uncertainty associated to the line-shape model (amounting to 54 kHz) was calculated as the root-mean-square value of the deviations of the line-center frequencies from the HTP value. The effect of the temperature uncertainty ($\Delta T \approx 0.15$ K) was of the order of 7 kHz. This quantity was calculated as the variation in the retrieved line-center frequency when setting the temperature at $T \pm \Delta T$. In a similar way, we quoted the influence of the uncertainty (± 3 MHz) on the zero-pressure center frequency of the HDO line. As far as the frequency scale is concerned, the quoted uncertainty is mostly due to the stability of the Rb clock. Other sources of systematical deviations, including the hyperfine structure, the detector nonlinearity, and the ac-Stark shift, were found to be negligible. The combined uncertainty result is 109 kHz. Such an absolute accuracy represents an improvement by a factor of 275 with respect to the previous CRDS determination under the Doppler-limited regime [7].

In Fig. 4, our value is compared with the recent determinations of Refs. [10,11] and with the theoretical values of Refs. [8,11]. The inset focuses attention on the experimental values; here, the error bars correspond to three times the measurement uncertainty. As for the comparison with calculations including QED, our value is roughly 7 MHz larger than the theoretical value of Ref. [11], namely, 217 105 174.8 $\pm$ 1.8 MHz. Instead, it is close to the value 217 105 180 $\pm$ 6 MHz that can be determined from Ref. [8].

IV. CONCLUSIONS

In conclusion, we have determined the absolute center frequency of the R(1) line of the HD (2,0) overtone band. Retrieved after a refined spectral analysis of high-quality absorption spectra, our value agrees with the recent sub-Doppler determination of Ref. [10] within 3σ, while it deviates about -1.2 MHz from the one of Tao *et al.* [11]. Finally, a highly precise value for the transition electric dipole moment was derived from the measured line strength, showing good agreement with the calculations of Pachucki and Komasa [9].

[1] J. Tumlinson, A. L. Malec, R. F. Carswell, M. T. Murphy, R. Buning, N. Milutinovic, S. L. Ellison, J. X. Prochaska, R. A. Jorgenson, W. Ubachs, and A. M. Wolfe, Astrophys. J. Lett. **718**, L156 (2010).
[2] D. A. Varshalovich, A. V. Ivanchik, P. Petitjean, R. Srianand, and C. Ledoux, Astron. Lett. **27**, 683 (2001).
[3] T. I. Ivanov, M. Roudjane, M. O. Vieitez, C. A. de Lange, W.-U. L. Tchang-Brillet, and W. Ubachs, Phys. Rev. Lett. **100**, 093007 (2008).
[4] E. J. Salumbides, J. C. J. Koelemeij, J. Komasa, K. Pachucki, K. S. E. Eikema, and W. Ubachs, Phys. Rev. D **87**, 112008 (2013).
[5] M. P. Ledbetter, M. V. Romalis, and D. F. Jackson Kimball, Phys. Rev. Lett. **110**, 040402 (2013).
[6] G. Herzberg, Nature (London) **166**, 563 (1950).
[7] S. Kassi and A. Campargue, J. Mol. Spectrosc. **267**, 36 (2011).
[8] K. Pachucki and J. Komasa, Phys. Chem. Chem. Phys. **12**, 9188 (2010).
[9] K. Pachucki and J. Komasa, Phys. Rev. A **78**, 052503 (2008).
[10] F. M. J. Cozijn, P. Dupré, E. J. Salumbides, K. S. E. Eikema, and W. Ubachs, Phys. Rev. Lett. **120**, 153002 (2018).
[11] L.-G. Tao, A.-W. Liu, K. Pachucki, J. Komasa, Y. R. Sun, J. Wang, and S.-M. Hu, Phys. Rev. Lett. **120**, 153001 (2018).
[12] E. Fasci, T. A. Odintsova, A. Castrillo, M. D. De Vizia, A. Merlone, F. Bertiglia, L. Moretti, and L. Gianfrani, Phys. Rev. A **93**, 042513 (2016).
[13] H. Dinesan, E. Fasci, A. D'Addio, A. Castrillo, and L. Gianfrani, Opt. Express **23**, 1757 (2015).
[14] O. Votava, M. Masat, A. E. Parker, C. Jain, and C. Fittschen, Rev. Sci. Instrum. **83**, 043110 (2012).
[15] P. Wcisło, I. E. Gordon, C.-F. Cheng, S.-M. Hu, and R. Ciuryło, Phys. Rev. A **93**, 022501 (2016).
[16] J. Tennyson, P. F. Bernath, A. Campargue, A. G. Császár, L. Daumont, R. R. Gamache, J. T. Hodges, D. Lisak, O. V. Naumenko, L. S. Rothman, H. Tran, N. F. Zobov, J. Buldyreva, C. D. Boone, M. D. D. Vizia, L. Gianfrani, J.-M. Hartmann, R. McPheat, D. Weidmann, J. Murray, N. H.

Ngo, and O. L. Polyansky, Pure Appl. Chem. **86**, 1931 (2014).

[17] N. Ngo, D. Lisak, H. Tran, and J.-M. Hartmann, J. Quant. Spectrosc. Radiat. Transf. **129**, 89 (2013).

[18] M. D. De Vizia, A. Castrillo, E. Fasci, L. Moretti, F. Rohart, and L. Gianfrani, Phys. Rev. A **85**, 062512 (2012).

[19] P. Amodio, L. Moretti, A. Castrillo, and L. Gianfrani, J. Chem. Phys. **140**, 044310 (2014).

[20] I. Gordon, L. Rothman, C. Hill, R. Kochanov, Y. Tan, P. Bernath, M. Birk, V. Boudon, A. Campargue, K. Chance, B. Drouin, J.-M. Flaud, R. Gamache, J. Hodges, D. Jacquemart, V. Perevalov, A. Perrin, K. Shine, M.-A. Smith, J. Tennyson, G. Toon, H. Tran, V. Tyuterev, A. Barbe, A. Csaszar, V. Devi, T. Furtenbacher, J. Harrison, J.-M. Hartmann, A. Jolly, T. Johnson, T. Karman, I. Kleiner, A. Kyuberis, J. Loos, O. Lyulin, S. Massie, S. Mikhailenko, N. Moazzen-Ahmadi, H. Muller, O. Naumenko, A. Nikitin, O. Polyansky, M. Rey, M. Rotger, S. Sharpe, K. Sung, E. Starikova, S. Tashkun, J. V. Auwera, G. Wagner, J. Wilzewski, P. Wcislo, S. Yu, and E. Zak, J. Quant. Spectrosc. Radiat. Transf. **203**, 3 (2017).

[21] N. Rich, J. Johns, and A. McKellar, J. Mol. Spectrosc. **95**, 432 (1982).